Research Article | Vol. 12, No. 5 / 1 May 2021 / Biomedical Optics Express 2825
Biomedical Optics EXPRESS

Quantification of intermittent retinal capillary perfusion in sickle cell disease

DAVIS B. ZHOU,[1,2] MARIA V. CASTANOS,[1] ALEXANDER PINHAS,[1] PETER GILLETTE,[3] JUSTIN V. MIGACZ,[1] RICHARD B. ROSEN,[1,2] JEFFREY GLASSBERG,[4] AND TOCO Y. P. CHUI[1,2,*]

[1] *Ophthalmology, New York Eye and Ear Infirmary of Mount Sinai, 310 East 14th St., Suite 500, S. Bldg., New York, NY 10003, USA*
[2] *Ophthalmology, Icahn School of Medicine at Mount Sinai, 1 Gustave L. Levy Pl, New York, NY 10029, USA*
[3] *Internal Medicine, SUNY Downstate Medical Center, 450 Clarkson Avenue Brooklyn, NY 11203, USA*
[4] *Emergency Medicine, Icahn School of Medicine at Mount Sinai, 3 East 101st Street, Box 1620, New York, NY 10029, USA*
[*] *ychui@nyee.edu*

Abstract: Pathophysiology of sickle cell disease (SCD) features intermittent vaso-occlusion of microcirculatory networks that facilitate ischemic damage. Past research has, however, relied on static images to characterize this active disease state. This study develops imaging metrics to more fully capture dynamic vascular changes, quantifying intermittent retinal capillary perfusion in unaffected controls and SCD patients using sequential optical coherence tomography angiography (OCT-A) scans. The results reveal significant dynamic variation of capillary perfusion in SCD patients compared to controls. This measurement of vaso-occlusive burden in patients would provide utility in monitoring of the disease state and in evaluating treatment efficacy.

1. Introduction

Sickle cell disease (SCD) is a group of autosomal-recessive gene mutations that alter the 3-dimensional folding of hemoglobin, the oxygen-carrying protein within erythrocytes [1,2]. Misfolded hemoglobin becomes susceptible to polymerization, which not only modifies erythrocyte morphology, but also leads to changes in signaling between erythrocytes, leukocytes, platelets, endotheliocytes, and additional elements of the blood clotting cascade [3–5]. These elements contribute together to increase vascular blockage [3–5]. This vaso-occlusion is considered a hallmark of SCD pathophysiology and is more likely to occur during cellular hypoxia and metabolic stress [6–8]. Vaso-occlusive events throughout the circulatory system lead to chronic inflammation, vessel remodeling, and ischemic end-organ damage [9,10], resulting in significant morbidity at an early age (including pain crises, acute chest syndrome, bone necrosis, myocardial infarction, and stroke) and early mortality in SCD patients [11–13].

The transparent media of the eye offers a unique opportunity to directly visualize the retinal microvasculature, as an indirect representation of the microvascular status of other organ systems. Correlations between retinal microvascular pathology and other systemic manifestations of diabetes, hypertension, and hypercholesterolemia, such as kidney disease, heart disease, myocardial infarction, and stroke, have been well established [14–16]. For instance, the correlation of hemoglobin A1c levels and degree of diabetic retinopathy through serial retinal exams has led to the establishment of diabetes treatment protocols for primary care physicians and endocrinologists [17,18]. Studying the retinal microvasculature in SCD patients may enable clinicians to use the retina as a conduit for assessing SCD vaso-occlusive risk and monitoring response to treatment.

#418874 https://doi.org/10.1364/BOE.418874
Journal © 2021 Received 30 Dec 2020; revised 13 Apr 2021; accepted 14 Apr 2021; published 21 Apr 2021

Biomedical Optics EXPRESS

Traditional classifications of sickle cell retinopathy in the clinical setting have mostly focused on the peripheral retina and its relatively later-stage microvascular complications, including permanent capillary closure and non-perfusion, subsequent collateralization and neovascularization, and sight-threatening vitreous hemorrhage and tractional retinal detachment [19]. Wide field fundus photography and intravenous fluorescein angiography (IV-FA) have emerged as the gold standard for characterizing these later-stage microvascular complications. These techniques have been used to characterize sickle cell retinopathy in the macula and temporal retina, including microaneurysms, hairpin venular loops, and capillary rarefaction, and enlargement of the foveal avascular zone [20–24]. They have also revealed intermittent vascular non-perfusion and reperfusion over intervals of days to months at the macula and temporal retina, showing *in vivo* the natural history of vaso-occlusive events and documenting the long-term remodeling and ischemic damage that occurs in sickle cell retinopathy [25–28]. Such modalities, however, are restricted to visualizing the superficial capillary network and are incapable of capturing dynamic microvascular vaso-occlusive events due to limitations in axial and transverse resolution [29]. Optical coherence tomography (OCT) has emerged as non-invasive imaging modality that offers micrometer axial and transverse resolution. Studies utilizing this technology have demonstrated both macular and temporal inner retinal thinning in SCD patients. Furthermore, subclinical signs of sickle cell maculopathy have been detected in patients with normal visual acuity using other functional indicators of disease such as contrast sensitivity, color vision, and microperimetry [30–32].

Optical coherence tomography angiography (OCT-A) builds upon on OCT to visualize perfused vasculature, enabled by differences in signal scattering from moving erythrocytes compared to surrounding tissue. Its quick image acquisition time and non-invasive nature allows OCT-A to accurately, reliably, and reproducibly image the retinal microvasculature at all capillary plexus depths across short and long time intervals [33–38]. OCT-A has allowed a closer examination of sickle cell retinopathy, permitting quantitative cross-sectional analysis of decreased microvascular density at both the macula and temporal retina compared to unaffected controls [24,39–41]. Existing OCT-A studies, however, often utilize single scans. Vessels considered perfused during initial scans might appear occluded upon repeat imaging due to intermittent vaso-occlusion. In this study, we thus explore a novel method for measuring disease status and response to systemic therapy by quantifying dynamic changes in intermittent capillary perfusion. These alternations were measured over minute intervals within imaging sessions and over a 1-hour interval between imaging sessions.

2. Methods

2.1. Subjects

This study was completed at the New York Eye and Ear Infirmary of Mount Sinai with approval by the Institutional Review Board of the Icahn School of Medicine at Mount Sinai. Patients were enrolled according to the tenants of the Declaration of Helsinki using written consent prior to imaging.

Inclusion criteria for unaffected controls were natural crystalline lens, clear media, steady fixation, and best corrected visual acuity (BCVA) of 20/20 or better. Inclusion criteria for patients were diagnosis of SCD, crystalline lens, and BCVA of 20/80 or better. Exclusion criteria for all participants were anterior segment pathology, previous refractive surgery, pseudophakia, cataract with grade ≥ 3, poor fixation, nystagmus, and retinal or optic disc pathology from other causes (e.g. diabetes, glaucoma, hypertension, retinal vein occlusion, or HIV). Only one eye was selected randomly from each participant.

Biomedical Optics EXPRESS

2.2. Image acquisition

OCT-A scans were acquired at two imaging sessions one hour apart using a spectral-domain OCT device, which features an illumination source centered at 840nm, a bandwidth of 45nm, an axial resolution of 5µm, and an acquisition rate of 70,000 A-scans per second (Avanti RTVue-XR; AngioAnalytics software version 2017.1.0; Optovue, Fremont, CA, USA). Vascular perfusion was assessed using the split-spectrum amplitude-decorrelation angiography algorithm on two orthogonally acquired volumes, which were subsequently merged to generate each OCT-A scan [35]. At each imaging session, 10 sequential 3×3mm (304×304pixel) OCT-A scans were acquired at two retinal locations: 1) the parafovea and 2) temporal retina centered 9 degrees eccentric to the fovea. In brief, each participant received a total of 40 OCT-A scans with 20 scans of the parafovea and 20 scans of the temporal retina.

One treatment-naïve SCD patient with HbSS genotype was imaged at an initial visit following the protocol described above and again two months after receiving an individualized dosage of 13.6 mg/kg of hydroxyurea using the same protocol, for a total of 80 OCT-A scans over the course of the study.

2.3. Image registration and averaging

At each retinal location, OCT-A scans were registered and averaged using the Register Virtual Stack Slices plug-in on ImageJ (ImageJ, U.S. National Institute of Health, Bethesda, Maryland, USA) [42,43]. OCT-A analysis was performed on the full vascular slab of each image, which included the inner limiting membrane to 9µm below the posterior boundary of the outer plexiform layer (Fig. 1(A)). This full vascular slab insured the inclusion of three different capillary networks including the superficial, intermediate, and deep capillary plexuses. OCT-A scan dimension was corrected based on individual axial length measurements obtained from the IOL Master (Carl Zeiss Meditec, Inc., Dublin, CA) to permit accurate comparison of vascular metrics between subjects [44].

2.4. Between-session pixel intensity difference in unaffected controls

Non-capillary areas of averaged OCT-A scans were excluded from the computation of pixel intensity difference between two sessions in unaffected controls (Fig. 1(B)). First, the foveal avascular zone (FAZ) was removed by demarcating the FAZ border manually on the averaged parafoveal OCT-A scan (Adobe Photoshop CS6, Adobe Systems, Inc., San Jose, CA, USA). Next, the removal of larger vessels using global thresholding was performed on both parafoveal and temporal retina averaged OCT-As as described previously (MATLAB 2018b; MathWorks, Natick, MA) [45,46].

Between-session pixel intensity difference was determined by subtracting the baseline averaged OCT-A from the 1-hour follow-up averaged OCT-A in each control (Fig. 1(C)). A positive pixel intensity difference indicates that intensity at the 1-hour follow-up was higher than during the baseline image, while a negative difference indicates that intensity at the 1-hour follow-up was lower than during the baseline image. Between-session pixel intensity differences of the parafoveal and temporal retina for all controls was then examined separately using Bland-Altman analysis. Between-session pixel intensity difference corresponding to the limits of agreement (LOA) between the 0.01^{st} percentile and 99.99^{th} percentile were defined as the normal range of between-session pixel intensity variation (Fig. 2).

2.5. Between-session intermittent perfusion index (IPI) in unaffected controls and SCD patients

Between-session intermittent perfusion index (IPI) was then determined for controls and SCD patients. First, the differences in pixel intensity were calculated between the baseline and 1-hour

Biomedical Optics EXPRESS

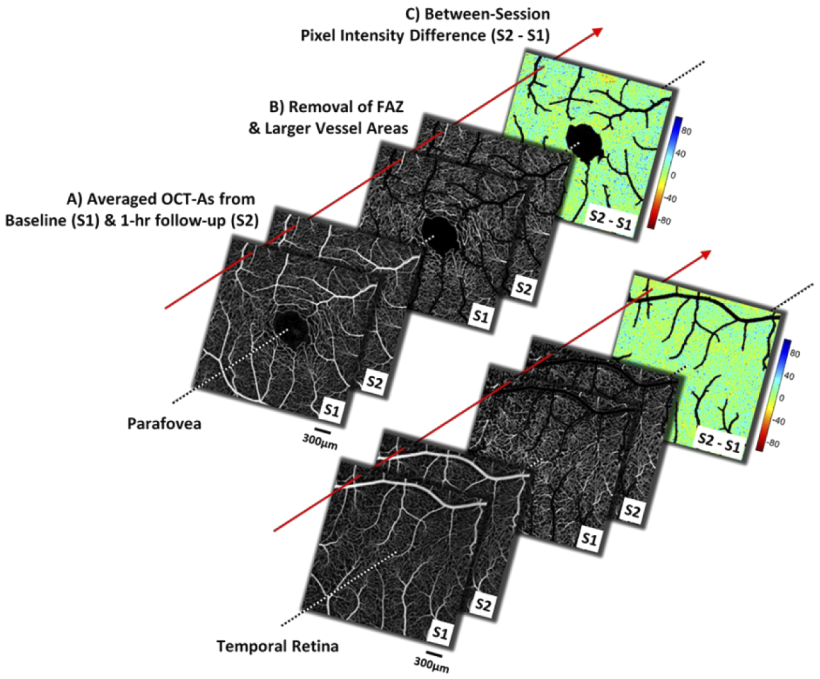

Fig. 1. Computation of between-session pixel intensity differences at the parafovea (top row) and temporal retina (bottom row) in an unaffected control. (A) Averaged full vascular slab OCT-As from baseline and 1-hour follow-up sessions. (B) Foveal avascular zone (FAZ) and larger vessel areas were removed from the OCT-As. FAZ area removal was performed on the parafoveal OCT-As only. (C) Between-session pixel intensity differences were then computed by subtracting baseline OCT-A (S1) from 1-hour follow-up OCT-A (S2). Positive pixel intensity difference (cool colors) indicates that pixel intensity at the follow-up session was higher than during the baseline, while a negative difference (warm colors) indicates that pixel intensity at the 1-hour follow-up was lower than during the baseline. FAZ and larger vessel areas are coded in black. Red arrows point to the same pixel location across panels. Measurements from unaffected controls were used to determine the normal variation in pixel intensity difference between sessions.

follow-up imaging sessions as described in Fig. 1. Pixels at which the difference in pixel intensity was outside the normal range of between-session pixel intensity variation in controls were defined as regions of intermittent perfusion. Specifically, the sum of pixels with intensity differences below the 0.01^{st} percentile were defined as areas of non-perfusion, indicating perfused capillaries at the baseline imaging session that lost perfusion at the 1-hour follow-up. In contrast, sum of pixels with intensity differences above the 99.99^{th} percentile were considered as regions of re-perfusion between sessions, indicating capillary areas without perfusion at the baseline that gained perfusion at the 1-hour follow-up.

Between-session IPI was defined as the percent of the entire OCT-A demonstrating non-perfusion and re-perfusion after the removal of FAZ and larger vessel areas. The removal of FAZ area was applied to the parafoveal OCT-A scans only.

$$\text{Between-Session IPI},\% = \frac{\text{Non-perfusion area} + \text{Re-perfusion area}}{\text{Total OCT-A area} - \text{FAZ area} - \text{Larger vessel area}} \times 100\%$$

Biomedical Optics EXPRESS

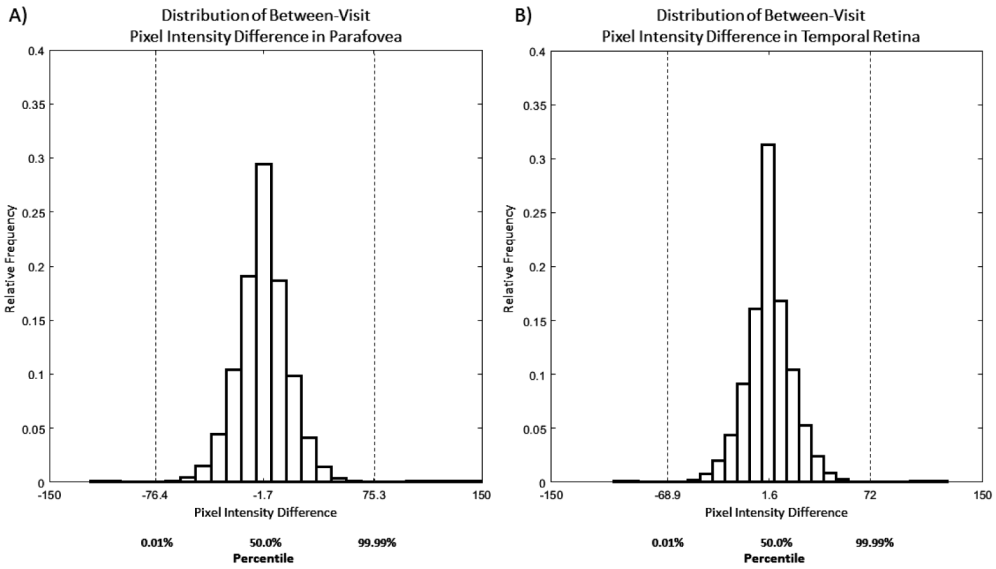

Fig. 2. Distribution of pixel intensity difference between the baseline and 1-hour follow-up visits in control subjects at the parafovea (A) and temporal retina (B). Limits of agreement at the 0.01% and 99.99% were calculated for controls and used to determine the normal pixel intensity variation in averaged OCT-A over the 1-hour interval. A positive pixel intensity difference indicates that intensity at the 1-hour follow-up was higher than during the baseline image, while a negative difference indicates that intensity at the 1-hour follow-up was lower than during the baseline image. The region in which the pixel intensity was below the lower limit of agreement (0.01%) was defined as non-perfusion and the area above upper limit of agreement (99.99%) was defined as re-perfusion.

2.6. Mapping of capillary segments with between-session intermittent perfusion

Intermittent perfusion maps were also generated for each subject to allow rapid visualization of perfusion changes between sessions. Capillary segments with intermittent perfusion between the baseline and follow-up sessions were overlaid on the averaged OCT-A of the two imaging sessions (S1 and S2 from Fig. 1). Segments demonstrating subsequent non-perfusion were highlighted in red and those exhibiting subsequent re-perfusion were displayed in cyan.

2.7. Within-session intermittent capillary perfusion

Within-session intermittent perfusion was qualitatively identified surrounding the FAZ for controls and SCD patients during the baseline and 1-hour follow-up imaging sessions. In each group of 10 sequential OCT-A scans, capillary segments exhibiting within-session intermittent perfusion were defined as those perfused in at least one OCT-A scan but demonstrating non-perfusion during a prior or subsequent scan [47]. The mean number of these capillary segments identified at the two imaging sessions was then calculated.

2.8. Capillary perfusion densities

Capillary perfusion density measurements were determined for comparison to existing OCT-A analyses. To calculate this metric, perfused capillaries were segmented from OCT-A scans using local thresholding after removal of the FAZ and non-capillary areas as described previously [34,45,46]. Parafoveal and temporal retina capillary perfusion densities (%) at each imaging session were then computed as described below. The removal of FAZ area was applied to the

Biomedical Optics EXPRESS

parafoveal capillary perfusion density computations only.

$$\text{Capillary Perfusion Density},\% = \frac{\text{Capillary area}}{\text{Total OCT-A area} - \text{FAZ area} - \text{Larger vessel area}} \times 100\%$$

2.9. Statistical analysis

For statistical analysis, SCD patients were divided into three subgroups according to their genotypes and hydroxyurea treatment status. The groups were 1) HbSC genotype without prior treatment, 2) HbSS genotype with hydroxyurea treatment, and 3) HbSS genotype without prior treatment. Between-session IPI, within-session intermittent perfusion, and capillary perfusion density in control and SCD subgroups were compared using Kruskal-Wallis with post-hoc pairwise comparisons. The percent areas of non-perfusion and re-perfusion measured between the baseline and 1-hour follow-up were compared in all groups using the Wilcoxon signed-rank test. All statistical tests were performed with SPSS 27 (IBM Corporation, Chicago, IL, USA).

3. Results

3.1. Demographics

A total of 14 unaffected controls and 13 SCD patients were enrolled in the study. One SCD patient was unable to complete the temporal retina imaging protocol at the 1-hour follow-up imaging session due to a prior personal commitment. Participant characteristics are displayed in Table 1. Percentages of female subjects were 36% and 54% respectively for control and SCD subgroups. Median ± IQR (interquartile range) age of controls and SCD subjects were respectively 27 ± 5 and 31 ± 14 years. Patients and controls were not matched by race, gender, or age. SCD genotypes included 8 patients with HbSS, 4 with HbSC, and 1 with sickle cell trait. Among patients with HbSS, 4 had been receiving treatment with hydroxyurea and 1 had received gene therapy. Patients with HbSC and sickle cell trait had no prior treatment history. The sickle cell trait patient and HbSS patient with gene therapy were excluded from the statistical analyses.

3.2. Between-session intermittent perfusion index (IPI) in unaffected controls and SCD patients

At the parafovea, between-session IPI of unaffected controls was 0.01 ± 0.03% (median ± IQR), with non-perfusion area of 0.005 ± 0.02% of the capillary area and re-perfusion area of 0.002 ± 0.007% of the area (Table 2). No statistical difference was found between the percent area with non-perfusion and re-perfusion on Wilcoxon Signed Rank test (P = 0.68) (Fig. 3(A)).

Between-session IPI of all SCD patients at the parafovea was 0.36 ± 0.72% (median ± IQR), with non-perfusion area of 0.20 ± 0.39% and re-perfusion area 0.16 ± 0.37% (Table 2). No statistical difference was found between the percent area non-perfusion and re-perfusion on Wilcoxon Signed Rank test (P = 0.25). Between-session IPI was 0.12 ± 0.2% for patients with the HbSC genotype, 0.52 ± 0.39 for the HbSS genotype with hydroxyurea treatment, and 2.59 ± 1.00 for the HbSS genotype without prior treatment (Table 2). In each SCD subgroup, no statistical difference was found between the percent area with non-perfusion and re-perfusion on Wilcoxon Signed Rank test (P values > 0.07) (Fig. 3(A)).

Statistically significant difference was observed among controls and SCD subgroups in between-session IPI using non-parametric Kruskal-Wallis test (P=0.001) (Fig. 4(A)). Significant differences for the post-hoc pairwise comparisons after non-parametric Kruskal-Wallis tests were found in controls vs HbSS with hydroxyurea treatment (P=0.027) and controls vs HbSS without prior treatment (P=0.004) only.

At the temporal retina, between-session IPI of unaffected controls was 0.02 ± 0.02% (median ± IQR), with non-perfusion area of 0.01 ± 0.02% and re-perfusion area of 0.01 ± 0.02% (Table 2). No statistical difference was found between the percent area with non-perfusion

Biomedical Optics EXPRESS

Table 1. Subject Characteristics

Characteristic	Result
Number of control subjects	14
• Age: median ± IQR (interquartile range)	27 ± 5 years
• Female: number (%)	5 (36%)
• Stratified by race	
– Caucasian	6 (42.9%)
– Hispanic	5 (35.7%)
– Asian	3 (21.4%)
Number of patients with sickle cell disease	13
• Age: median ± IQR	31 ± 14 years
• Female: number (%)	7 (54%)
• Stratified by genotype	
– HbSS	8 (61.5%)
– HbSC	4 (30.8%)
– Sickle Cell Trait	1 (7.7%)
• Stratified by race	
– African American	11 (84.6%)
– Hispanic	2 (15.4%)
• Prior Treatment	
– Hydroxyurea	4 (30.8%)
– Gene therapy	1 (7.7%)
– Intraocular Anti-VEGF Injection	0 (0.0%)

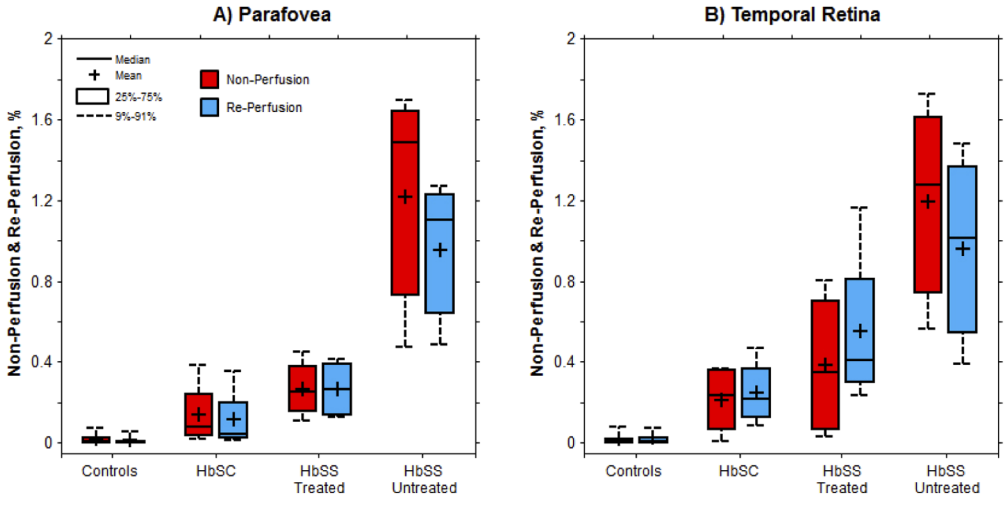

Fig. 3. Boxplots of percent area non-perfusion and re-perfusion areas in controls and SCD subgroups at the parafovea (A) and temporal retina (B). No statistically significant differences were found between the percent area non-perfusion and re-perfusion on Wilcoxon Signed Rank test in all groups (All P values >0.05). The sickle cell trait patient and HbSS patient with gene therapy were excluded from the statistical analyses.

Biomedical Optics EXPRESS

Table 2. Between-session intermittent capillary perfusion in controls and SCD subgroups. Tx = Treatment; NA = data not available.

	Parafovea (median ± IQR %)			Temporal (median ± IQR %)		
	Between-session IPI	Non-perfusion area	Re-perfusion area	Between-session IPI	Non-perfusion area	Re-perfusion area
Controls, n=14	0.01 ± 0.03	0.005 ± 0.02	0.002 ± 0.007	0.02 ± 0.02	0.01 ± 0.02	0.01 ± 0.02
All SCD, n=13	0.36 ± 0.72	0.20 ± 0.39	0.16 ± 0.37	0.58 ± 0.97	0.36 ± 0.56	0.38 ± 0.39
SCD Subgroups						
Sickle cell trait without Tx, n=1	0.009	0.005	0.004	0.022	0.006	0.016
HbSC without Tx, n=4	0.12 ± 0.2	0.08 ± 0.12	0.05 ± 0.09	0.50 ± 0.1	0.24 ± 0.3	0.22 ± 0.2
HbSS with Hydroxyurea Tx, n=4	0.52 ± 0.39	0.25 ± 0.16	0.26 ± 0.23	0.86 ± 1.0	0.35 ± 0.6	0.41 ± 0.3
HbSS with gene therapy, n=1	0.16	0.05	0.11	NA	NA	NA
HbSS without Tx, n=3	2.59 ± 1.00	1.49 ± 0.61	1.10 ± 0.39	2.74 ± 0.9	1.28 ± 0.6	1.01 ± 0.5

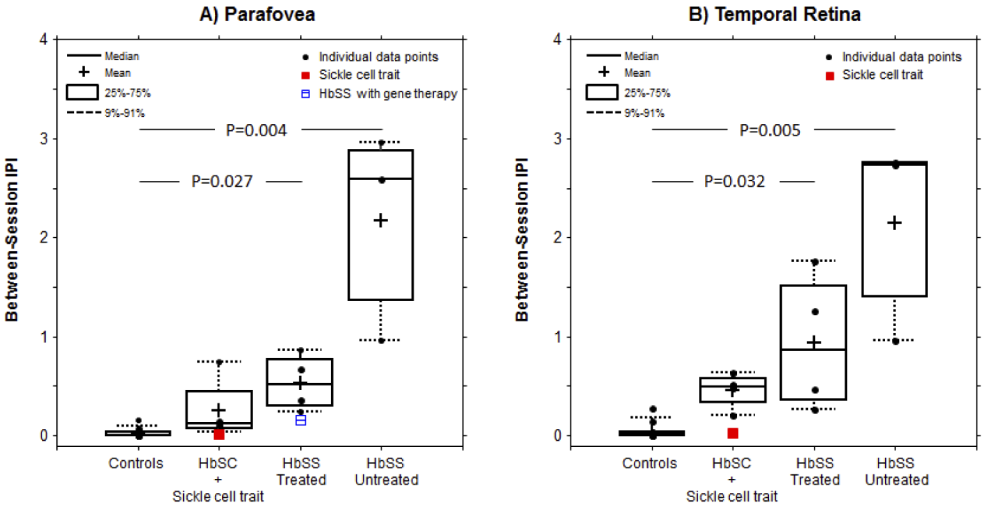

Fig. 4. Boxplots of between-session IPI in control and SCD subgroups at the parafovea (A) and temporal retina (B). Statistically significant differences were observed among 4 groups at the parafovea (P=0.001) and temporal retina (P<0.001) using non-parametric Kruskal-Wallis tests. Significant P-values for the post-hoc pairwise comparisons after nonparametric Kruskal-Wallis tests are shown; all other comparisons were not significant (P > 0.05). The sickle cell trait patient (red square) and HbSS patient with gene therapy (blue square) were excluded from the statistical analyses.

Biomedical Optics EXPRESS

and re-perfusion on Wilcoxon Signed Rank test (P = 1.0) (Fig. 3(B)). In all SCD patients, between-session IPI was 0.58 ± 0.97% (median ± IQR), with non-perfusion area of 0.36 ± 0.56% and re-perfusion area of 0.38 ± 0.39% (Table 2). No statistical difference was found between the percent area with non-perfusion and re-perfusion on Wilcoxon Signed Rank test (P = 0.75). Between-session IPI was 0.50 ± 0.1 for patients having the HbSC genotype, 0.86 ± 1.0 for the HbSS genotype with hydroxyurea treatment, and 2.74 ± 0.9 for the HbSS genotype without prior treatment (Table 2).

Statistically significant differences were observed among controls and SCD subgroups for between-session IPI using non-parametric Kruskal-Wallis tests (P<0.001) (Fig. 4(B)). Significant P-values for the post-hoc pairwise comparisons after non-parametric Kruskal-Wallis tests were found in controls vs HbSS with hydroxyurea treatment (P=0.032) and controls vs HbSS without prior treatment (P=0.005) only.

3.3. *Mapping of capillary segments with between-session intermittent perfusion*

Intermittent perfusion maps provide an accessible representation of between-session capillary perfusion changes for clinical use. Figure 5 shows averaged OCT-A scans and intermittent perfusion maps in a SCD patient with HbSC genotype at the parafovea (top row) and temporal retina (bottom row) for the baseline and 1-hour follow-up imaging sessions. Direct visualization of capillary segments with non-perfusion (red) and re-perfusion (cyan) between the baseline and 1-hour follow-up are shown in the intermittent perfusion maps.

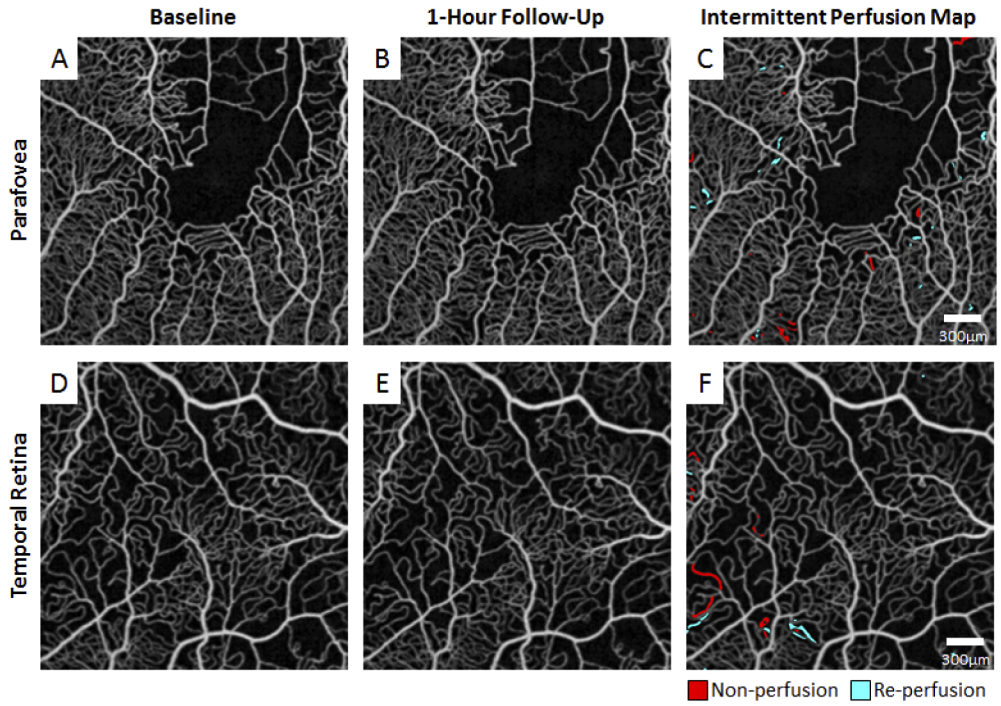

Fig. 5. Averaged OCT-A of a SCD patient with HbSC genotype at the parafovea (top row) and temporal retina (bottom row) for the baseline (A & D) and 1-hour follow-up (B & E) imaging sessions. Visualization of capillary segments with non-perfusion (red) and re-perfusion (cyan) between the baseline and 1-hour follow-up were shown in the intermittent perfusion maps at the parafovea (C) and temporal retina (F).

Biomedical Optics EXPRESS

Intermittent perfusion maps also aid the immediate identification and evaluation of capillaries with between-session intermittent perfusion before and after treatment. In the treatment-naïve SCD patient with HbSS genotype who began hydroxyurea, between-session IPI was 3.0% and 2.7% respectively at the parafovea and temporal retina before treatment. After two months of hydroxyurea, the between-session IPI was reduced to 0.5% and 1.6% respectively at the parafovea and temporal retina (Fig. 6).

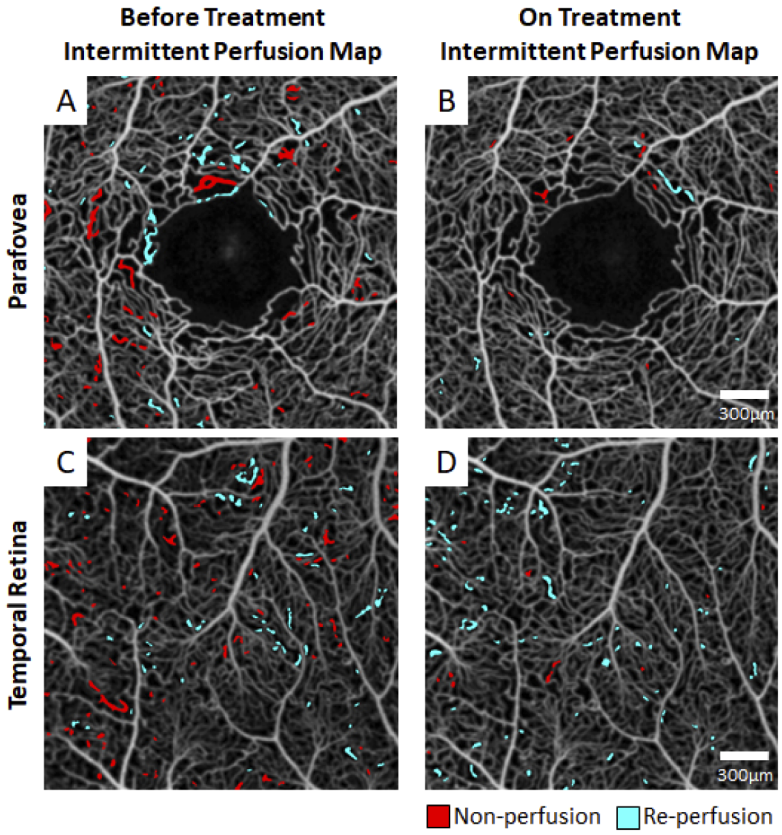

Fig. 6. A treatment naïve SCD patient with HbSS genotype was imaged at an initial visit (left column) and repeated imaging again after two months of hydroxyurea treatment (right column). Before treatment, the patient exhibited between-session IPI of 3.0% and 2.7% respectively at the parafovea (A) and temporal retina (C). After two months of hydroxyurea, the between-session IPI was reduced to 0.5% and 1.6% respectively at the parafovea (B) and temporal retina (D).

3.4. Within-session intermittent capillary perfusion

Intermittent perfusion within at least one imaging session was seen surrounding the FAZ in 4 of 14 controls and in all 13 SCD patients. Figure 7 shows an example of within-session intermittent capillary perfusion in a SCD patient with HbSS genotype and hydroxyurea treatment (also see Visualization 1). Within-session intermittent capillary perfusion was seen in 0.25 ± 0.43 (mean ± SD) capillary segments for controls and 3.1 ± 2.2 segments for all SCD patients. Within-session intermittent capillary perfusion was seen in 2.0 ± 0.6 capillary segments for SCD patients having the HbSC genotype, 2.9 ± 1.1 segments for the HbSS genotype with hydroxyurea treatment, and 5.7 ± 3.6 segments for the HbSS genotype without prior treatment.

Biomedical Optics EXPRESS

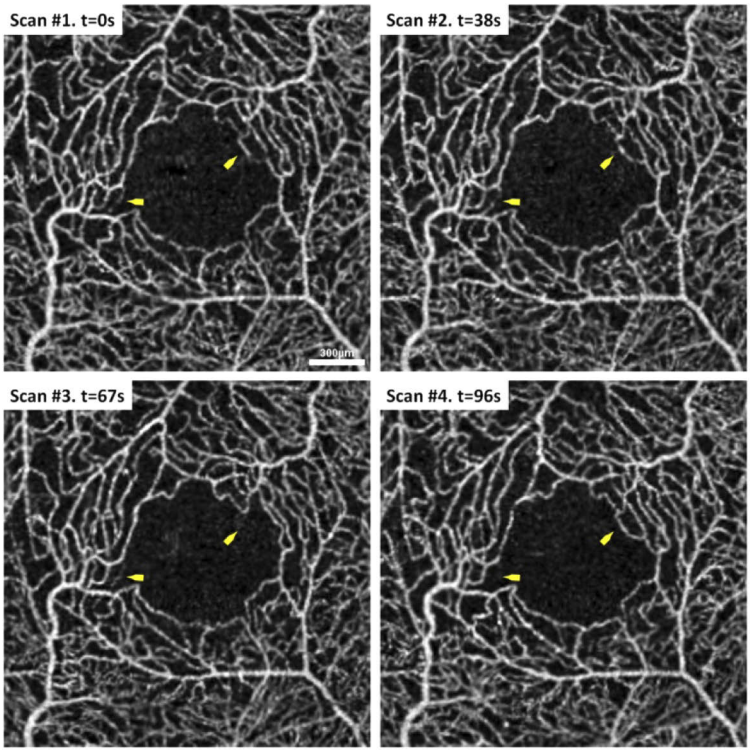

Fig. 7. Within-session intermittent capillary perfusion in a SCD HbSS patient with hydroxyurea treatment. Yellow arrows indicate two capillary segments bordering the FAZ with intermittent capillary perfusion at the first four OCT-A scans during the baseline imaging session (see Visualization 1 for all ten frames). Corresponding time of image acquisition was indicated on the upper left corner of each OCT-A scan.

Statistical significance was observed among controls and SCD subgroups using non-parametric Kruskal-Wallis tests ($P<0.001$). Significant P-values for the post-hoc pairwise comparisons were found in controls vs HbSC without prior treatment ($P=0.05$), controls vs HbSS with hydroxyurea treatment ($P=0.008$), and controls vs HbSS without prior treatment ($P=0.009$) only. In the treatment-naïve SCD patient with HbSS genotype who began hydroxyurea, within-session intermittent perfusion surrounding the FAZ prior to treatment was seen in an average of 8 capillary segments prior to treatment and an average of 3.5 segments after two months of hydroxyurea therapy.

3.5. Capillary perfusion densities

In unaffected controls, capillary perfusion density (median ± IQR) at the parafovea was similar between the baseline ($51.0 \pm 0.4\%$) and 1-hour follow-up ($51.2 \pm 0.3\%$) imaging sessions, without significance on Wilcoxon Signed Rank test ($P=0.07$). Capillary perfusion density among all SCD patients (median ± IQR) at the parafovea was also comparable between the baseline ($49.1 \pm 3.5\%$) and 1-hour follow-up ($49.3 \pm 3.6\%$) imaging sessions, without significance on Wilcoxon Signed Rank test ($P=0.16$). Statistically significant difference was observed among controls and SCD subgroups in capillary perfusion density (mean of baseline and 1-hour follow-up) at the parafovea using non-parametric Kruskal-Wallis test ($P=0.002$). Significant P-value for the post-hoc pairwise comparisons after non-parametric Kruskal-Wallis tests was found in controls vs HbSS with hydroxyurea treatment ($P=0.01$) only. There was no significant difference among controls and

Biomedical Optics EXPRESS

SCD subgroups in capillary perfusion density (mean of baseline and 1-hour follow-up) at the temporal retina using non-parametric Kruskal-Wallis test (P=0.079).

4. Discussion

Using IV-FA, Galinos et al. in 1975 first documented non-perfusion and subsequent re-perfusion of retinal vessels in sickle cell retinopathy over several months [26]. Intermittent perfusion of shorter periods (over days duration) was subsequently reported by Asdourian et al. in 1976 [25]. In our study, sequential OCT-A scans revealed intermittent capillary perfusion at intervals of minutes to hours.

4.1. Between-session intermittent perfusion index (IPI) in unaffected controls and SCD patients

Intermittent flow maps revealed vascular changes over time in SCD patients despite capillary perfusion density showing similar measurements across the 1-hour imaging sessions. This is likely due to the finding that areas of non-perfusion and re-perfusion were of similar magnitudes, which underscored the importance of our new proposed methodology to detect changes. These observations may also suggest an ability of microvasculature to compensate for small alterations in perfusion.

We believe that intermittent perfusion measurements provide unique characterization of dynamic vaso-occlusion in retinal microvascular networks. Previous sickle cell retinopathy imaging studies using fundoscopy, IV-FA, and OCT-A have relied on single scans, basing their clinical evaluations on cross-sectional static pictures of a dynamic pathophysiology. Their findings of retinal thinning on OCT and decreased capillary perfusion density on OCT-A were limited to describing cumulative vascular and tissue damage from chronic ischemia, rather than the active nature of intermittent vaso-occlusive events. This ability to characterize dynamic vaso-occlusion more accurately and quantifiably depicts ongoing disease burden and severity of SCD for a given individual. Isolating non-perfusion and re-perfusion of individual capillary segments may thus prove more useful for predicting progression of retinal and systemic manifestations of the disease. These intermittent perfusion changes on sequential OCT-A have recently been shown to correspond to retinal capillary segments with erythrocyte sludging or stasis using adaptive optics scanning light ophthalmoscopy (Pinhas and Migacz et al. IOVS 2020:6; ARVO E-Abstract 1928).

Importantly, intermittent perfusion measurements appear useful for evaluating efficacy of systemic treatment in SCD. Hydroxyurea is currently the best systemic medical therapy available for reducing painful vaso-occlusive crises and all-cause mortality in patients, through its ability to promote production of fetal hemoglobin, limit leukocyte-erythrocyte interactions, and donate nitric oxide [48,49]. Lower levels of intermittent perfusion were detected both within and between sessions in patients with HbSS receiving hydroxyurea compared to those without hydroxyurea treatment. Additionally, a treatment naïve patient with HbSS demonstrated decreased within-session intermittent perfusion at the parafovea after 2 months of treatment with hydroxyurea. This patient also exhibited reduced between-session IPI after treatment (from 3.0% to 0.54% of the capillary area at the parafovea and from 2.7% to 1.6% of the capillary area at the temporal retina). Such results are consistent with a recent longitudinal study suggesting the protective effect of hydroxyurea on rates of retinal thinning in patients with sickle cell retinopathy [50]. Greater stability of retinal perfusion – as characterized by lower between-session IPI – may help explain the reduced retinal thinning found in the patients receiving hydroxyurea. Overall, our findings suggest that intermittent perfusion analysis may be a more sensitive biomarker, compared to OCT retinal thickness and OCT-A capillary density, for detecting and quantifying otherwise occult areas of non-perfusion and re-perfusion, as well as measuring response to systemic treatment in SCD.

Biomedical Optics EXPRESS

4.2. Within-session intermittent capillary perfusion

Within-session perfusion change in capillaries bordering the FAZ over minutes was seen in every SCD patient, at statistically significant higher rates than in unaffected controls. Changes in between-session intermittent perfusion were also seen in SCD patients, when comparing baseline imaging to 1-hour follow-up imaging. These alterations in between-session IPI, percent area of non-perfusion, and percent area of re-perfusion at both the parafovea and temporal retina were statistically greater in SCD patients compared to unaffected controls.

4.3. Limitations

Limitations of the study include the unmatched age, race, and gender differences between the control and patient groups. Age has been shown to correlate with decreased retinal vascular density [51]. In contrast, lower vascular perfusion density has been documented for individuals with greater retinal pigmentation, which may be more common in certain racial groups [52]. In addition, limitations in sample size, particularly of patients with SCD, prevented statistical analysis of intermittent perfusion between patient subgroups e.g. sick cell trait. Notably, analysis was also performed on a full retinal vascular slab in order to reduce any impact of projection artifacts on OCT-A or OCT segmentation error. The use of this combined layer, however, prevented the ability to compare differences in intermittent perfusion between capillary plexuses. Finally, ten OCT-A scans were obtained at each imaging location in order to measure within-session capillary perfusion changes and generate averaged scans for between-session alterations. Thus, clinical application of this scan protocol would require patients with stable fixation and tolerance of the longer acquisition time.

4.4. Future directions

Future directions of this research include prospective investigation of intermittent capillary perfusion in larger populations of patients before and after hydroxyurea treatment, which would more thoroughly characterize the impact of systemic therapy. New SCD therapies have also emerged that merit evaluation for their impact on the microvascular mechanisms of disease [53–55]. Subsequent studies with increased sample size would also permit the comparison of intermittent capillary perfusion between disease subtypes and in relation to hematological metrics of SCD, such as hematocrit, lactate dehydrogenase, and platelet count. These studies would further evaluate intermittent capillary perfusion as a means for monitoring disease pathophysiology and quantifying treatment effects.

5. Conclusion

In summary, intermittent perfusion measurement and mapping enables quantification and rapid identification of intermittent retinal capillary perfusion events in SCD patients. Intermittent perfusion events were significantly more frequent in SCD than in unaffected controls. They are evident over intervals of minutes as well as hours on sequential OCT-A, which suggests an important clarification of sickle cell vaso-occlusion pathophysiology. Intermittent perfusion quantification and mapping technique also shows promise for evaluation of treatment effect, given its ability to detect variations of intermittent perfusion seen in response to systemic hydroxyurea therapy.

Funding. Challenge Grant Award from Research to Prevent Blindness; Jorge N. Buxton Microsurgical Foundation; Marrus Family Foundation; New York Eye and Ear Infirmary Foundation; National Institutes of Health (R01EY027301).

Acknowledgments. The content is solely the responsibility of the authors and does not necessarily represent the official views of the National Institutes of Health.

Disclosures. Richard B. Rosen: OptoVue: Code C (Consultant) & Code P (Patent) ; Boehringer-Ingelheim: Code C (Consultant); Astellas: Code C; Genentech-Roche: Code C; NanoRetina: Code C; OD-OS: Code C; Opticology: Code I

Biomedical Optics EXPRESS

(Personal Financial Interest); Guardion: Code I (Personal Financial Interest); GlaucoHealth: Code I (Personal Financial Interest); Regeneron: Code C (Consultant); Bayer: Code C (Consultant); Teva: Code C (Consultant).

Jeffrey Glassberg: Global Blood Therapeutics (Consultant), Pfizer (Contracted Research), CSL Behring (Consultant)

References

1. A. Driss, K. O. Asare, J. M. Hibbert, B. E. Gee, T. V. Adamkiewicz, and J. K. Stiles, "Sickle cell disease in the post genomic era: a monogenic disease with a polygenic phenotype," Genomics Insights **2**, GEI.S2626 (2009).
2. W. A. Eaton and J. Hofrichter, "The biophysics of sickle cell hydroxyurea therapy," Science **268**(5214), 1142–1143 (1995).
3. R. Hoover, R. Rubin, G. Wise, and R. Warren, "Adhesion of normal and sickle erythrocytes to endothelial monolayer cultures," Blood **54**(4), 872–876 (1979).
4. D. K. Kaul, M. E. Fabry, and R. L. Nagel, "Microvascular sites and characteristics of sickle cell adhesion to vascular endothelium in shear flow conditions: pathophysiological implications," Proc. Natl. Acad. Sci. **86**(9), 3356–3360 (1989).
5. R. A. Swerlick, J. R. Eckman, A. Kumar, M. Jeitler, and T. M. Wick, "Alpha 4 beta 1-integrin expression on sickle reticulocytes: vascular cell adhesion molecule-1-dependent binding to endothelium," Blood **82**(6), 1891–1899 (1993).
6. R. P. Hebbel, O. Yamada, C. F. Moldow, H. S. Jacob, J. G. White, and J. W. Eaton, "Abnormal adherence of sickle erythrocytes to cultured vascular endothelium: possible mechanism for microvascular occlusion in sickle cell disease," J. Clin. Invest. **65**(1), 154–160 (1980).
7. D. K. Kaul, M. E. Fabry, P. Windisch, S. Baez, and R. L. Nagel, "Erythrocytes in sickle cell anemia are heterogeneous in their rheological and hemodynamic characteristics," J. Clin. Invest. **72**(1), 22–31 (1983).
8. P. C. Hines, Q. Zen, S. N. Burney, D. A. Shea, K. I. Ataga, E. P. Orringer, M. J. Telen, and L. V. Parise, "Novel epinephrine and cyclic AMP-mediated activation of BCAM/Lu-dependent sickle (SS) RBC adhesion," Blood **101**(8), 3281–3287 (2003).
9. D. C. Rees, T. N. Williams, and M. T. Gladwin, "Sickle-cell disease," Lancet **376**(9757), 2018–2031 (2010).
10. D. K. Kaul and R. P. Hebbel, "Hypoxia/reoxygenation causes inflammatory response in transgenic sickle mice but not in normal mice," J. Clin. Invest. **106**(3), 411–420 (2000).
11. O. S. Platt, D. J. Brambilla, W. F. Rosse, P. F. Milner, O. Castro, M. H. Steinberg, and P. P. Klug, "Mortality in sickle cell disease–life expectancy and risk factors for early death," N Engl J Med **330**(23), 1639–1644 (1994).
12. H. M. Haupt, G. W. Moore, T. W. Bauer, and G. M. Hutchins, "The lung in sickle cell disease," Chest **81**(3), 332–337 (1982).
13. S. Charache and D. L. Page, "Infarction of bone marrow in the sickle cell disorders," Ann. Intern. Med. **67**(6), 1195–1200 (1967).
14. J. E. Grunwald, J. Alexander, G.-S. Ying, M. Maguire, E. Daniel, R. Whittock-Martin, C. Parker, K. McWilliams, J. C. Lo, A. Go, R. Townsend, C. A. Gadegbeku, J. P. Lash, J. C. Fink, M. Rahman, H. Feldman, J. W. Kusek, D. Xie, B. G. Jaar, and f. t. Cric Study Group, "Retinopathy and chronic kidney disease in the chronic renal insufficiency cohort (CRIC) study," Arch. Ophthalmol. **130**(9), 1136–1144 (2012).
15. P. O'sullivan, N. Hickey, B. Maurer, P. Guinan, and R. Mulcahy, "Retinal artery changes correlated with other hypertensive parameters in a coronary heart disease case-history study," Heart **30**(4), 556–562 (1968).
16. R. Poplin, A. V. Varadarajan, K. Blumer, Y. Liu, M. V. McConnell, G. S. Corrado, L. Peng, and D. R. Webster, "Prediction of cardiovascular risk factors from retinal fundus photographs via deep learning," Nat. Biomed. Eng. **2**(3), 158–164 (2018).
17. T. D. R. Group, "The diabetes control and complications trial (DCCT). Design and methodologic considerations for the feasibility phase," Diabetes **35**(5), 530–545 (1986).
18. U. K. P. D. S. Group, "UK prospective diabetes study (UKPDS)," Diabetologia **34**(12), 877–890 (1991).
19. A. W. Scott, "Ophthalmic manifestations of sickle cell disease," South Med. J. **109**(9), 542–548 (2016).
20. M. H. Goldbaum, "Retinal depression sign indicating a small retinal infarct," Am. J. Ophthalmol. **86**(1), 45–55 (1978).
21. T. S. Stevens, B. Busse, C.-B. Lee, M. B. Woolf, S. O. Galinos, and M. F. Goldberg, "Sickling hemoglobinopathies: macular and perimacular vascular abnormalities," Arch. Ophthalmol. **92**(6), 455–463 (1974).
22. F. Menaa, B. A. Khan, B. Uzair, and A. Menaa, "Sickle cell retinopathy: improving care with a multidisciplinary approach," JMDH **10**, 335–346 (2017).
23. S. Grover, K. Sambhav, and K. V. Chalam, "Capillary nonperfusion by novel technology of OCT angiography in a patient with sickle cell disease with normal fluorescein angiogram," Eur. J. Ophthalmol. **26**(5), e121–e123 (2016).
24. I. C. Han, M. Tadarati, and A. W. Scott, "Macular vascular abnormalities identified by optical coherence tomographic angiography in patients with sickle cell disease," JAMA Ophthalmol. **133**(11), 1337–1340 (2015).
25. G. K. Asdourian, K. C. Nagpal, B. Busse, M. Goldbaum, D. Patriankos, M. F. Rabb, and M. F. Goldberg, "Macular and perimacular vascular remodelling sickling haemoglobinopathies," Br. J. Ophthalmol. **60**(6), 431–453 (1976).
26. S. O. Galinos, G. K. Asdourian, M. B. Woolf, T. S. Stevens, C.-B. Lee, M. F. Goldberg, J. C. F. Chow, and B. J. Busse, "Spontaneous remodeling of the peripheral retinal vasculature in sickling disorders," Am. J. Ophthalmol. **79**(5), 853–870 (1975).

Biomedical Optics EXPRESS

27. I. Acacio and M. F. Goldberg, "Peripapillary and macular vessel occlusions in sickle cell anemia," Am. J. Ophthalmol. **75**(5), 861–866 (1973).
28. A. Mantovani and I. Figini, "Sickle cell-hemoglobin C retinopathy: transient obstruction of retinal and choroidal circulations and transient drying out of retinal neovessels," Int. Ophthalmol. **28**(2), 135–137 (2008).
29. D. A. Pahl, N. S. Green, M. Bhatia, and R. W. S. Chen, "New ways to detect pediatric sickle cell retinopathy: a comprehensive review," J. Pediatr. Hematol. Oncol. **39**(8), 618–625 (2017).
30. G. C. Martin, C. Dénier, O. Zambrowski, D. Grévent, L. Bruère, V. Brousse, M. de Montalembert, D. Brémond-Gignac, and M. P. Robert, "Visual function in asymptomatic patients with homozygous sickle cell disease and temporal macular atrophy," JAMA Ophthalmol. **135**(10), 1100–1105 (2017).
31. M. S. Roy, G. Rodgers, R. Gunkel, C. Noguchi, and A. Schechter, "Color vision defects in sickle cell anemia," Arch. Ophthalmol. **105**(12), 1676–1678 (1987).
32. C. C. Chow, M. A. Genead, A. Anastasakis, F. Y. Chau, G. A. Fishman, and J. I. Lim, "Structural and functional correlation in sickle cell retinopathy using spectral-domain optical coherence tomography and scanning laser ophthalmoscope microperimetry," Am. J. Ophthalmol. **152**(4), 704–711.e2 (2011).
33. I. C. Han, M. Tadarati, K. D. Pacheco, and A. W. Scott, "Evaluation of macular vascular abnormalities identified by optical coherence tomography angiography in sickle cell disease," Am. J. Ophthalmol. **177**, 90–99 (2017).
34. G. Lynch, A. W. Scott, M. O. Linz, I. Han, J. S. Andrade Romo, R. E. Linderman, J. Carroll, R. B. Rosen, and T. Y. Chui, "Foveal avascular zone morphology and parafoveal capillary perfusion in sickle cell retinopathy," Br. J. Ophthalmol. **104**(4), 473–479 (2020).
35. Y. Jia, O. Tan, J. Tokayer, B. Potsaid, Y. Wang, J. J. Liu, M. F. Kraus, H. Subhash, J. G. Fujimoto, J. Hornegger, and D. Huang, "Split-spectrum amplitude-decorrelation angiography with optical coherence tomography," Opt. Express **20**(4), 4710–4725 (2012).
36. D. B. Zhou, A. W. Scott, M. O. Linz, I. C. Han, M. V. Castanos, G. Lynch, J. S. Andrade Romo, R. E. Linderman, J. Carroll, R. B. Rosen, and T. Y. Chui, "Interocular asymmetry of foveal avascular zone morphology and parafoveal capillary density in sickle cell retinopathy," PLoS ONE **15**(6), e0234151 (2020).
37. T. E. De Carlo, A. Romano, N. K. Waheed, and J. S. Duker, "A review of optical coherence tomography angiography (OCTA)," Int. J. Retin. Vitr. **1**(1), 5 (2015).
38. K. R. Mendis, C. Balaratnasingam, P. Yu, C. J. Barry, I. L. McAllister, S. J. Cringle, and D.-Y. Yu, "Correlation of histologic and clinical images to determine the diagnostic value of fluorescein angiography for studying retinal capillary detail," Invest. Ophthalmol. Vis. Sci. **51**(11), 5864–5869 (2010).
39. Q. V. Hoang, F. Y. Chau, M. Shahidi, and J. I. Lim, "Central macular splaying and outer retinal thinning in asymptomatic sickle cell patients by spectral-domain optical coherence tomography," Am. J. Ophthalmol. **151**(6), 990–994 (2011).
40. K. Sambhav, S. Grover, and K. V. Chalam, "Temporal thinning in sickle cell retinopathy is associated with diminished perfusion on OCTA and dense scotoma on microperimetery," Retin Cases Brief Rep. **13**, 308–313 (2017).
41. R. K. Murthy, S. Grover, and K. V. Chalam, "Temporal macular thinning on spectral-domain optical coherence tomography in proliferative sickle cell retinopathy," Arch. Ophthalmol. **129**(2), 247–249 (2011).
42. S. Mo, E. Phillips, B. D. Krawitz, R. Garg, S. Salim, L. S. Geyman, E. Efstathiadis, J. Carroll, R. B. Rosen, and T. Y. P. Chui, "Visualization of radial peripapillary capillaries using optical coherence tomography angiography: the effect of image averaging," PLoS ONE **12**(1), e0169385 (2017).
43. M. V. Castanos, D. B. Zhou, R. E. Linderman, R. Allison, T. Milman, J. Carroll, J. Migacz, R. B. Rosen, and T. Y. P. Chui, "Imaging of macrophage-like cells in living human retina using clinical OCT," Invest. Ophthalmol. Vis. Sci. **61**(6), 48 (2020).
44. D. M. Sampson, P. Gong, D. An, M. Menghini, A. Hansen, D. A. Mackey, D. D. Sampson, and F. K. Chen, "Axial length variation impacts on superficial retinal vessel density and foveal avascular zone area measurements using optical coherence tomography angiography," Invest. Ophthalmol. Vis. Sci. **58**(7), 3065–3072 (2017).
45. J. S. Andrade Romo, R. E. Linderman, A. Pinhas, J. Carroll, R. B. Rosen, and T. Y. P. Chui, "Novel development of parafoveal capillary density deviation mapping using an age-group and eccentricity matched normative OCT angiography database," Trans. Vis. Sci. Tech. **8**(3), 1 (2019).
46. N. K. Scripsema, P. M. Garcia, R. D. Bavier, T. Y. Chui, B. D. Krawitz, S. Mo, S. A. Agemy, L. Xu, Y. B. Lin, J. F. Panarelli, P. A. Sidoti, J. C. Tsai, and R. B. Rosen, "Optical coherence tomography angiography analysis of perfused peripapillary capillaries in primary open-angle glaucoma and normal-tension glaucoma," Invest. Ophthalmol. Vis. Sci. **57**(9), OCT611 (2016).
47. B. D. Krawitz, E. Phillips, R. D. Bavier, S. Mo, J. Carroll, R. B. Rosen, and T. Y. P. Chui, "Parafoveal nonperfusion analysis in diabetic retinopathy using optical coherence tomography angiography," Trans. Vis. Sci. Tech. **7**(4), 4 (2018).
48. S. Charache, M. L. Terrin, R. D. Moore, G. J. Dover, F. B. Barton, S. V. Eckert, R. P. McMahon, and D. R. Bonds, "Effect of hydroxyurea on the frequency of painful crises in sickle cell anemia," N. Engl. J. Med. **332**(20), 1317–1322 (1995).
49. M. H. Steinberg, F. Barton, O. Castro, C. H. Pegelow, S. K. Ballas, A. Kutlar, E. Orringer, R. Bellevue, N. Olivieri, J. Eckman, M. Varma, G. Ramirez, B. Adler, W. Smith, T. Carlos, K. Ataga, L. DeCastro, C. Bigelow, Y. Saunthararajah, M. Telfer, E. Vichinsky, S. Claster, S. Shurin, K. Bridges, M. Waclawiw, D. Bonds, and M. Terrin, "Effect of

Biomedical Optics EXPRESS

hydroxyurea on mortality and morbidity in adult sickle cell anemia: risks and benefits up to 9 years of treatment," JAMA **289**(13), 1645–1651 (2003).
50. J. I. Lim, M. Niec, J. Sun, and D. Cao, "Longitudinal assessment of retinal thinning in adults with and without sickle cell retinopathy using spectral-domain optical coherence tomography," JAMA Ophthalmol. **139**(3), 330–337 (2021).
51. Y. Wei, H. Jiang, Y. Shi, D. Qu, G. Gregori, F. Zheng, T. Rundek, and J. Wang, "Age-related alterations in the retinal microvasculature, microcirculation, and microstructure," Invest. Ophthalmol. Vis. Sci. **58**(9), 3804–3817 (2017).
52. L. Y. Chun, M. R. Silas, R. C. Dimitroyannis, K. Ho, and D. Skondra, "Differences in macular capillary parameters between healthy black and white subjects with optical coherence tomography angiography (OCTA)," PLoS ONE **14**, e0223142 (2019).
53. K. I. Ataga, A. Kutlar, J. Kanter, D. Liles, R. Cancado, J. Friedrisch, T. H. Guthrie, J. Knight-Madden, O. A. Alvarez, V. R. Gordeuk, S. Gualandro, M. P. Colella, W. R. Smith, S. A. Rollins, J. W. Stocker, and R. P. Rother, "Crizanlizumab for the prevention of pain crises in sickle cell disease," N. Engl. J. Med. **376**(5), 429–439 (2017).
54. Y. Niihara, S. T. Miller, J. Kanter, S. Lanzkron, W. R. Smith, L. L. Hsu, V. R. Gordeuk, K. Viswanathan, S. Sarnaik, I. Osunkwo, E. Guillaume, S. Sadanandan, L. Sieger, J. L. Lasky, E. H. Panosyan, O. A. Blake, T. N. New, R. Bellevue, L. T. Tran, R. L. Razon, C. W. Stark, L. D. Neumayr, and E. P. Vichinsky, "A phase 3 trial of L-glutamine in sickle cell disease," N. Engl. J. Med. **379**(3), 226–235 (2018).
55. E. Vichinsky, C. C. Hoppe, K. I. Ataga, R. E. Ware, V. Nduba, A. El-Beshlawy, H. Hassab, M. M. Achebe, S. Alkindi, R. C. Brown, D. L. Diuguid, P. Telfer, D. A. Tsitsikas, A. Elghandour, V. R. Gordeuk, J. Kanter, M. R. Abboud, J. Lehrer-Graiwer, M. Tonda, A. Intondi, B. Tong, and J. Howard, "A phase 3 randomized trial of voxelotor in sickle cell disease," N. Engl. J. Med. **381**(6), 509–519 (2019).